THE JOURNAL OF PHYSICAL CHEMISTRY Letters

Letter

pubs.acs.org/JPCL

Effects of Intermolecular Charge Transfer in Liquid Water on Raman Spectra

Hironobu Ito,* Taisuke Hasegawa,* and Yoshitaka Tanimura*

Department of Chemistry, Graduate School of Science, Kyoto University, Sakyoku, Kyoto 606-8502, Japan

Supporting Information

ABSTRACT: The low-frequency vibrational spectrum of liquid water is composed of contributions from the intermolecular librational and translation modes. The existence of these two modes introduces difficulty into the simulation of experimentally obtained Raman spectra. We constructed a polarizability function for a water model that includes intramolecular charge flow (CF) effects, intermolecular charge transfer (CT) effects, and intermolecular dipole-induced-dipole (DID) effects. We computed the one-dimensional (1D) Raman and terahertz (THz) spectra with all of these effects included (CFCT-DID) and compared with experimental spectra. We find that the CFCT-DID function provides a better description of the experimental results, because the CT effects reduce the polarizability only for translational motion to which parallelly polarized (VV) and perpendicularly polarized (VH) Raman spectra are sensitive. In our calculations of two-dimensional (2D) Raman and THz-Raman spectra, we observe the enhancement of echo signals in both cases. The details of the CFCT-DID function, along with its source code, are provided in the Supporting Information.

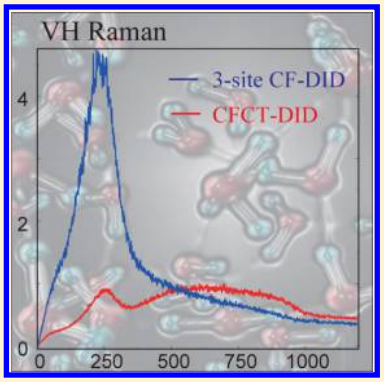

The chemical uniqueness of water, which depends strongly on complex hydrogen bonding, arises from the large polarizability of the water molecule.[1−3] Third-order off-resonant Raman spectroscopy, which exploits this polarizability, is a versatile tool for investigating the dynamics of complex hydrogen bond networks of water molecules.[4−12] This spectroscopic approach is suitable to investigate the collective intermolecular motion that spread over a spectral range below 1000 cm^{-1}.[13−17] Molecular dynamics (MD) simulations play an essential role in the analysis of experimentally obtained spectra.[18−22] While there are several studies investigating intermolecular charge transfer effects on IR spectra,[23,24] there are no studies investigating such effects on Raman spectra. In the present work, we developed a polarizability function that takes into account charge flow (CF), charge transfer (CT), and dipole-induced-dipole (DID) effects on the basis of a four-site water molecular model. We used this function to reproduce experimentally obtained Raman spectra with MD trajectories. Then, we examined the intermolecular CT effect on Raman spectra.

The CFCT-DID function is a polarizability function used to calculate the induced and charge transfer effects in the simulated system from given molecular trajectories that are calculated from the force fields in nonpolarizable potential models, for example TIP4P/2005. This function was developed on the basis of the full-order charge-flow and dipole-induced-dipole (CF-DID) function,[25−27] which was originally developed as a part of a polarizable water force field model for intermolecular and intramolecular vibrational spectroscopy (POLI2VS).[25] While the original CF-DID function is based on a three-site water model with two hydrogen atoms and one oxygen atom (the 3-site CF-DID function), we generalized it to a four-site case (the 4-site CF-DID function) in order to obtain a more accurate anisotropic profile of the molecular polarizability, which plays an important role in two-dimensional (2D) Raman[26−34] and 2D Raman−terahertz (THz)[26,27,34−39] spectroscopies. The CFCT-DID function further incorporates the intermolecular CT effect into the 4-cite CF-DID function, which is described by the CT polarizability, taking into account the charge transfer among the molecules (see Figure 1). By adding the CT polarizability to the CF polarizability as the charge−charge (CC) polarizability, $\alpha^{CF}_{i_kj_l} \rightarrow \alpha^{CC}_{i_kj_l} \equiv \alpha^{CF}_{i_kj_l} + \alpha^{CT}_{i_kj_l}$, we have developed the CFCT-DID function as an extension of the CF-DID function. Here, the CT polarizability is defined as $\alpha^{CT}_{i_kj_l} \equiv A_{kl} e^{-S_{kl} r_{i_kj_l}} / r_{i_kj_l}$ $(i \neq j)$, where A_{kl} and S_{kl} are the amplitude and screening parameters obtained from the computational results of *ab initio* calculations. In this function, the transferred charge from the kth site of the ith molecule due to the intermolecular CT effect is given by $q^{CT}_{i_k} = \sum_j \sum_l \alpha^{CT}_{i_kj_l} V_{j_l}$. The details of the CFCT-DID function with its source code are provided as Supporting Information.

In Figure 2, we display the dependences of the water dipole moments and polarizabilities on $r_{1_O 2_{H1}}$, the distance between the oxygen atom of Molecule 1 and the first hydrogen atom of Molecule 2 for the dimer conformation presented in Figure 1b, as obtained from the CFCT-DID function, the CF-DID function, and *ab initio* calculations. The *ab initio* calculations were carried out using the CCSD approach with the aug-cc-

Received: August 8, 2016
Accepted: September 30, 2016

DOI: 10.1021/acs.jpclett.6b01766
J. Phys. Chem. Lett. 2016, 7, 4147−4151

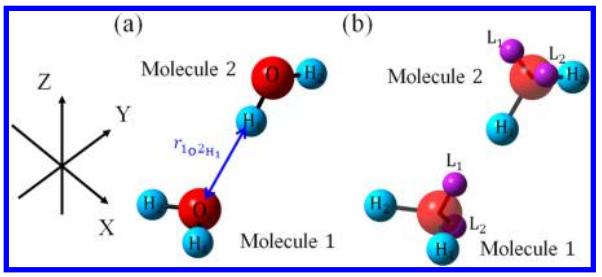

Figure 1. Depictions of the (a) 3-site CF-DID function and (b) 4-site CF-DID and CFCT-DID functions. The CF-DID functions utilize the dipole polarizability of the kth interaction site of the ith molecule, $\boldsymbol{\alpha}_{i_k}$, and the CF polarizability between the kth interaction site of the ith molecule and the lth interaction site of the jth molecule, $\alpha^{CF}_{i_k j_l}$, where k = H_1, H_2, and O for the 3-site case, and k = H_1, H_2, L_1, and L_2 for the 4-site case. The induced dipole moment, $\boldsymbol{\mu}^{I}_{i_k}$, and the induced charge, $q^{I}_{i_k}$, of the kth site of the ith molecule are given by $\boldsymbol{\mu}^{I}_{i_k} = \boldsymbol{\alpha}^{DD}_{i_k}\boldsymbol{E}_{i_k}$ and $q^{I}_{i_k} = \sum_l \alpha^{CF}_{i_k j_l} V_{i_k}$, where $\boldsymbol{E}_{i_k}$ and V_{i_k} are the electric field and potential of the kth site of the ith molecule, respectively. The CFCT-DID function further incorporates the intermolecular CT effect into the 4-cite CF-DID function, which is described by the CT polarizability, $\alpha^{CT}_{i_k j_l}$, taking into account the charge transfer among the molecules.

pVTZ basis set, employing the counterpoise method to correct for the basis set superposition error (BSSE). Both the CFCT-DID and CF-DID functions reproduce to the dipole moment calculated from *ab initio* calculation; however, the polarizability calculated from the CF-DID function is overestimated in comparison with *ab initio* calculation in panels c, e, and f. This is because the CF-DID function does not describe the attenuation of the electrostatic interactions at short distances accurately. Including the intermolecular CT effect, the CFCT-DID can more properly describe the overlap between electron densities in realistic situations.

In order to test the accuracy of our polarizability function, we next computed one-dimensional (1D) and two-dimensional (2D) spectra[26−39] using the CF-DID and CFCT-DID functions. To carry out the MD simulations for liquid water, we modeled the interactions between the molecules with TIP4P/2005.[40,41] We performed the MD simulations in a cubic box with periodic boundary conditions. We employed 216 molecules in the 1D case and 64 molecules in the 2D case. The volume and energy were fixed after the completion of isothermal simulations carried out to establish equilibration at approximately 300 K. The conditions of the simulation were chosen so as to realize an average density of 0.997 g/cm^3. The details of the numerical calculations are presented in the Supporting Information.

In Figure 3, we display (a) THz, (b) parallelly polarized (VV) Raman, and (c) perpendicularly polarized (VH) Raman spectra obtained from MD simulations and experiments. In the panels labeled (i), the red, green and blue curves represent the computational results obtained from the CFCT-DID (red curves), 4-site CF-DID (green curves), and 3-site CF-DID (blue) functions. The experimentally obtained THz,[42] VV, VH, and isotropic Raman spectra[43] are presented in the panel labeled (ii). To elucidate the contribution of the CT effect, in Figure 4, we decompose the 1D vibrational spectra calculated using the CFCT-DID function into the permanent-plus-induced (P+I) contribution and the CT contributions of the dipole and polarizability. (Detailed analysis is given in the Supporting Information.)

As shown in Figure 4a, because the effects of intermolecular CT are minor in comparison with those of the permanent and induced dipole moments, the peak profiles of the THz spectra computed using the CFCT-DID and CF-DID functions

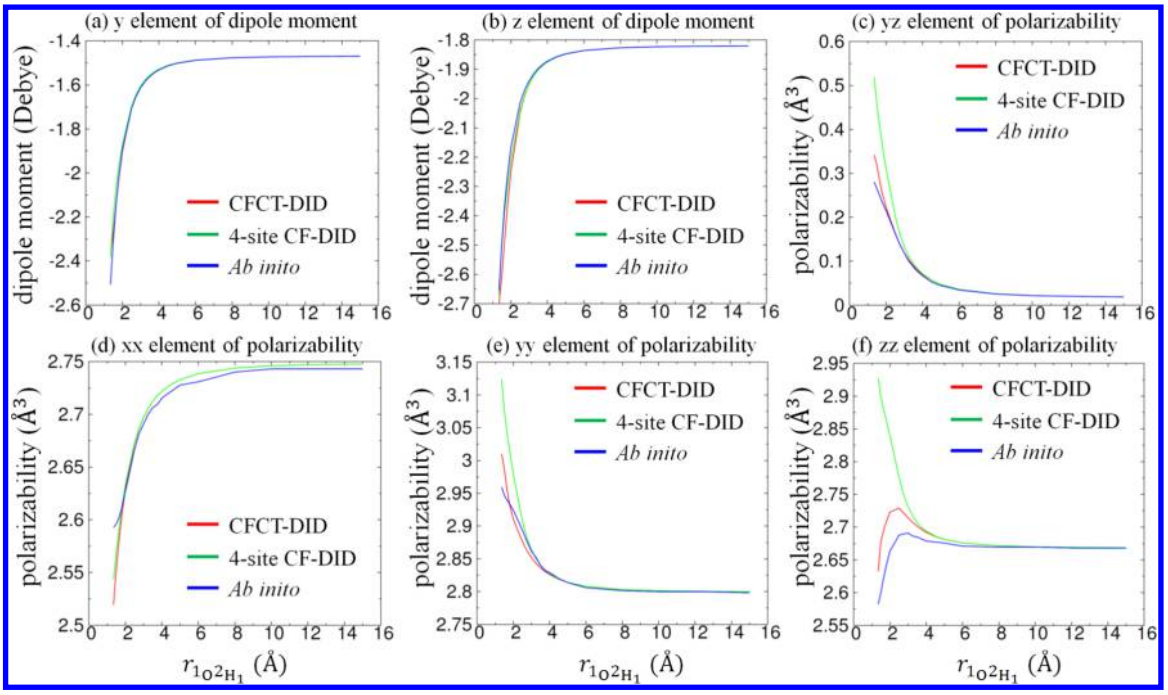

Figure 2. (a) Y and (b) z elements of the dipole moment, and the (c) yz, (d) xx (e) yy and (f) zz elements of the polarizability calculated using the CFCT-DID function (red curve), the CF-DID function (green curve), and the *ab initio* method (blue curve). The dipole and polarizabilities are defined in the molecular frame, as illustrated in Figure 1.

DOI: 10.1021/acs.jpclett.6b01766
J. Phys. Chem. Lett. 2016, 7, 4147−4151

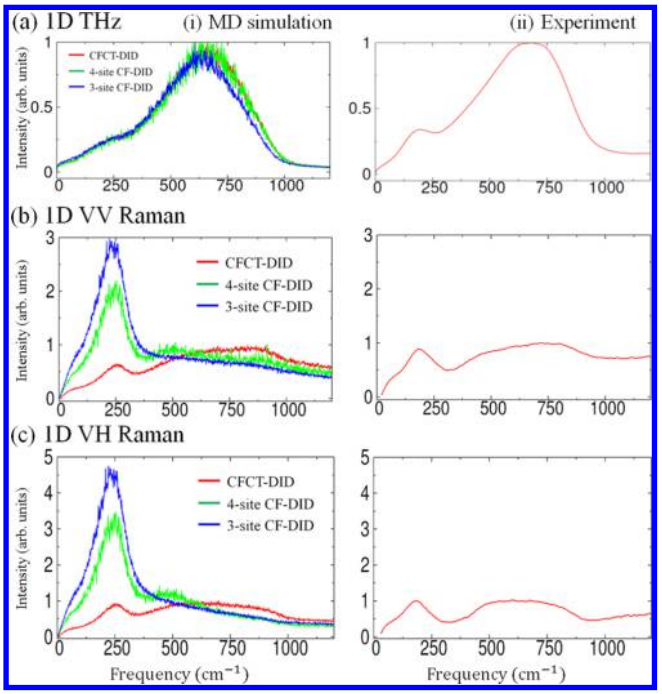

Figure 3. (a) THz, (b) parallelly polarized (VV) Raman, and (c) perpendicularly polarized (VH) Raman spectra obtained from (i) MD simulations and from (ii) experiments.[42,43] In the panels labeled (i), the red, green, and blue curves represent the computational results obtained from the CFCT-DID, 4-site CF-DID, and 3-site CF-DID functions, respectively.

appearing in Figure 3a are similar. While the CF-DID functions accurately reproduce the experimentally obtained THz spectrum, they fail to reproduce the VV and VH Raman spectra. In particular, in the results obtained from the CF-DID function, the peak for the librational modes, in the range 400−1000 cm^{-1}, is much weaker than that for the intermolecular translational modes, near 200 cm^{-1}, in contrast to the experimental situation. The results for the VV and VH Raman spectra obtained using the CFCT-DID approach are closer to the experimental results due to the intermolecular CT effect. The reason that the CFCT-DID function can improve the VV and VH spectra is that it is effective in capturing the physical nature of the CT process. The intermolecular CT process reduces the change in the polarizability by moving charge between the nearest neighbor molecules with the effects of increasing or decreasing the intermolecular distance. Translational motion alters the intermolecular distance, while librational motion alters the orientation. Thus, the peak intensity corresponding to translational motion, near 200 cm^{-1}, is suppressed by the CT effects, while that corresponding to librational motion, in the range 400−1000 cm^{-1}, does not change significantly. As a result, the overall profiles of the VV and VH spectra obtained with the CFCT-DID function presented in Figure 3b,c are closer to the experimental results than those obtained with the CF-DID functions.

In Figure 5, we present the (i) 2D Raman-THz-THz (RTT), (ii) 2D THz-Raman-THz (TRT), (iii) 2D THz-THz-Raman (TTR), and (iv) 2D Raman signals calculated using the (a) 3-site CF-DID function, (b) 4-site CF-DID function, and (c) CFCT-DID function, respectively. Because of the sensitivity of the optical properties probed in these 2D measurements, there are significant differences between the spectra obtained with the CFCT-DID and CF-DID functions, although no significant differences between the 3-site and 4-site functions are observed. The difference is most prominent in the 2D Raman case, because 2D Raman measurements involve three Raman excitations, while 2D THz-Raman measurements involve only one excitation. The echo contribution along the $t_1 = t_2$ direction in the 2D Raman and THz-Raman-THz spectra is larger in the CFCT-DID results than in the CF-DID results. The 2D profiles of these signals have been analyzed in terms of anharmonicity, nonlinear polarizability, and dephasing time.[39] These analysis indicate that the enhancement of echo signal occurs because the anisotropy of the CF effect strengthens the nonlinearity of the molecular polarizability, which plays an essential role in the second-rephasing excitation of 2D Raman and 2D THz-Raman measurements. Although CT effects are minor in comparison with CF effects, we observe an enhancement of the high-frequency peaks near the t_1 axis, corresponding to librational motion, as illustrated in the cases of the 1D VV and VH Raman spectra.

In this work, we constructed a CFCT-DID polarizability function, with intramolecular CF and intermolecular CT effects for using MD simulations of liquid water. With the CT effects included, this new function is an improvement over the CF-DID functions, producing results that are significantly closer to the experimental results. We also found that the CT effects enhance the nonlinear polarizability, which, in turn, enhances the echo contribution to signals in 2D THz-Raman-THz and 2D Raman spectra. Finally, we note that in this study, we used the same trajectories obtained with the TIP4P/2005 force field in both the CFCT-DID and CF-DID polarizability functions.

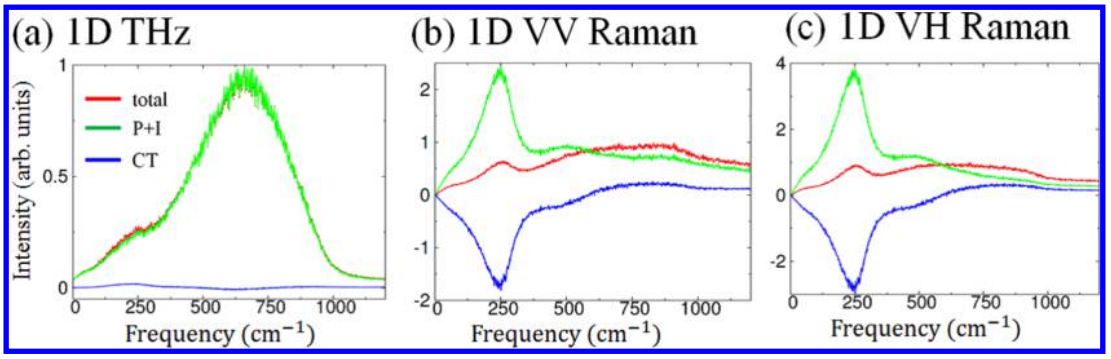

Figure 4. Computational results of (a) THz, (b) parallelly polarized (VV) Raman, and (c) perpendicularly polarized (VH) Raman spectra obtained from the CFCT-DID function. The total 1D THz and 1D Raman spectra are expressed in terms of the P+I and CT contributions of the dipole and polarizability. The spectral intensities are normalized with respect to the absolute value of the peak intensities of the total contribution.

DOI: 10.1021/acs.jpclett.6b01766
J. Phys. Chem. Lett. 2016, 7, 4147−4151

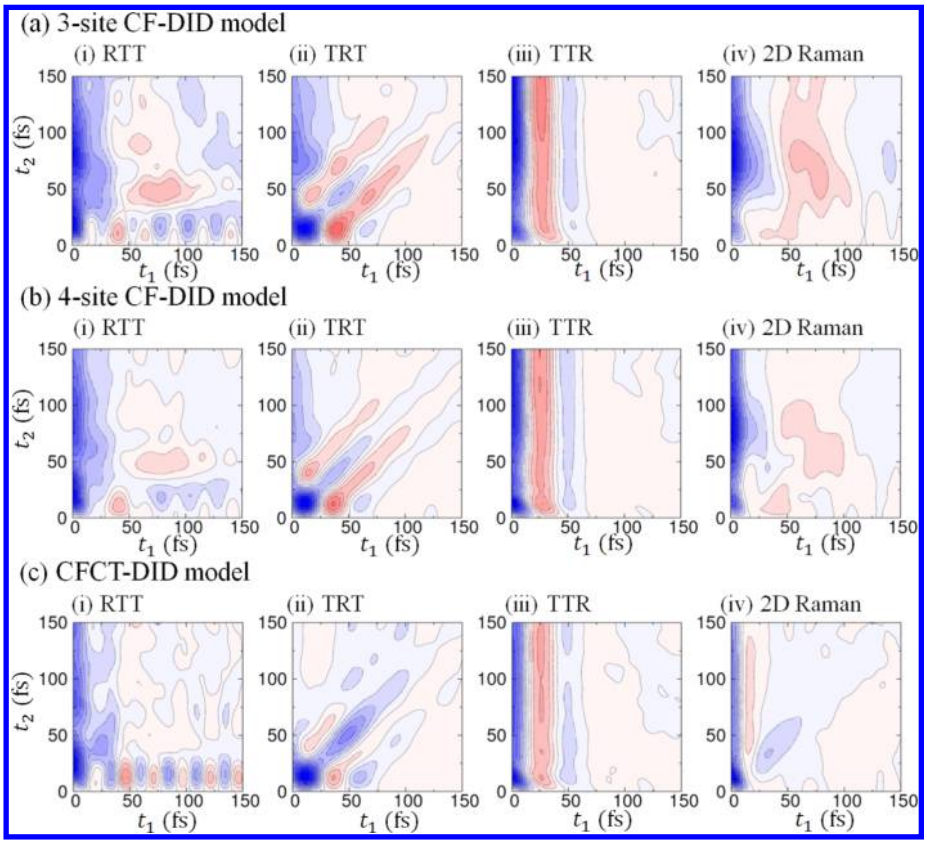

Figure 5. The zzzz tensor elements of (i) RTT, (ii) TRT, (iii) TTR signals, and the zzzzzz tensor elements of (iv) 2D Raman signals for liquid water calculated using the (a) CF-DID and (b) CFCT-DID functions. Red and blue shadings represent positive and negative signals, respectively. The signal intensities are normalized with respect to the absolute value of the peak signal intensities.

Thus, the suppression of the translational peaks in the VV and VH Raman spectra are not due to differences in intermolecular dynamics but to differences in the polarizability arising from the CT effect.

In the present paper, we showed that CT effects reduce the polarizability only for translational motion to which VV and VH Raman spectra are sensitive. This indicates that spectra for the librational motion of water obtained from the sum frequency generation (SFG) may not change significantly if we include CT effects.[44] It may be possible to test this hypothesis by incorporating the CFCT-DID function into the POLI2VS potential and calculating the SFG spectrum using the full MD simulation approach.

■ ASSOCIATED CONTENT

Supporting Information

The Supporting Information is available free of charge on the ACS Publications website at DOI: 10.1021/acs.jpclett.6b01766.

Details of the CFCT-DID polarization function (ZIP)

FORTRAN source code (ZIP)

■ AUTHOR INFORMATION

Corresponding Authors

*E-mail: h.ito@kuchem.kyoto-u.ac.jp.

*E-mail: hasegawa@kuchem.kyoto-u.ac.jp.

*E-mail: tanimura@kuchem.kyoto-u.ac.jp.

Notes

The authors declare no competing financial interest.

■ ACKNOWLEDGMENTS

This research is supported by a Grant-in-Aid for Scientific Research (A26248005) from the Japan Society for the Promotion of Science. Some of the computational resources used in this work were provided by the Research Center for Computational Science, Okazaki, Japan.

■ REFERENCES

(1) Eisenberg, D.; Kauzmann, W. *The Structures and Properties of Water*; Oxford University Press: New York, 1969.

(2) Franks, F. *Water: A Comprehensive Treatise*; Plenum Press: New York, 1972−1982; Vols. *1*−*7*.

(3) Robinson, G. W.; Singh, S.; Zhu, S.-B.; Evans, M. W. *Water in Biology, Chemistry and Physics*; World Scientific Press: Singapore, 1996.

(4) Walrafen, G. E.; Fisher, M. R.; Hokmabadi, M. S.; Yang, W. H. Temperature dependence of the low and high frequency Raman scattering from liquid water. *J. Chem. Phys.* **1986**, *85*, 6970−6982.

(5) Castner, E. W., Jr.; Chang, Y. J.; Chu, Y. C.; Walrafen, G. E. The intermolecular dynamics of liquid water. *J. Chem. Phys.* **1995**, *102*, 653−659.

(6) Fecko, C. J.; Eaves, J. D.; Tokmakoff, A. Isotropic and anisotropic Raman scattering from molecular liquids measured by spatially masked optical Kerr effect spectroscopy. *J. Chem. Phys.* **2002**, *117*, 1139−1154.

(7) Torre, T.; Bartolini, P.; Righini, R. Structural relaxation in supercooled water by time-resolved spectroscopy. *Nature* **2004**, *428*, 296−299.

(8) Fukasawa, T.; Sato, T.; Watanabe, J.; Hama, Y.; Kunz, W.; Buchner, R. Relation between Dielectric and Low-Frequency Raman Spectra of Hydrogen-Bond Liquids. *Phys. Rev. Lett.* **2005**, *95*, 197802.

(9) Hunt, N. T.; Kattner, L.; Shanks, R. P.; Wynne, K. The Dynamics of Water-Protein Interaction Studied by Ultrafast Optical Kerr-Effect Spectroscopy. *J. Am. Chem. Soc.* **2007**, *129*, 3168−3172.

DOI: 10.1021/acs.jpclett.6b01766
J. Phys. Chem. Lett. 2016, 7, 4147−4151

(10) Heisler, I. A.; Meech, S. R. Low-Frequency Modes of Aqueous Alkali Halide Solutions: Glimpsing the Hydrogen Bonding Vibration. *Science* **2010**, *327*, 857−860.
(11) Mazur, K.; Heisler, I. A.; Meech, S. R. Low-Frequency Modes of Aqueous Alkali Halide Solutions: An Ultrafast Optical Kerr Effect Study. *J. Phys. Chem. B* **2011**, *115*, 1863−1873.
(12) Taschin, A.; Bartolini, P.; Eramo, E.; Righini, R.; Torre, R. Evidence of two distinct local structures of water from ambient to supercooled conditions. *Nat. Commun.* **2013**, *4*, 2401.
(13) Ohmine, I.; Tanaka, H.; Wolynes, P. G. Large local energy fluctuations in water. II. Cooperative motions and fluctuations. *J. Chem. Phys.* **1988**, *89*, 5852−5860.
(14) Sasai, M.; Ramaswamy, R.; Ohmine, I. Long time fluctuation of liquid water: 1/f spectrum of energy fluctuation in hydrogen bond network rearrangement dynamics. *J. Chem. Phys.* **1992**, *96*, 3045−3053.
(15) Ohmine, I.; Tanaka, H. Fluctuation, Relaxations, and Hydration in Liquid Water. Hydrogen-Bond Rearrangement Dynamics. *Chem. Rev.* **1993**, *93*, 2545−2566.
(16) Ohmine, I. Liquid Water Dynamics: Collective Motions, Fluctuation, and Relaxation. *J. Phys. Chem.* **1995**, *99*, 6767−6776.
(17) Matsumoto, M.; Ohmine, I. A new approach to the dynamics of hydrogen bond network in liquid water. *J. Chem. Phys.* **1996**, *104*, 2705−2712.
(18) Cho, M.; Fleming, G. R.; Saito, S.; Ohmine, I.; Stratt, R. M. Instantaneous normal mode analysis of liquid water. *J. Chem. Phys.* **1994**, *100*, 6672−6683.
(19) Ohmine, I.; Saito, S. Water Dynamics: Fluctuation, Relaxation, and Chemical Reactions in Hydrogen Bond Network Rearrangement. *Acc. Chem. Res.* **1999**, *32*, 741−749.
(20) Imoto, S.; Xantheas, S.; Saito, S. Molecular origin of the difference in the HOH bend of the IR spectra between liquid water and ice. *J. Chem. Phys.* **2013**, *138*, 054506.
(21) Paesani, F.; Medders, G. R. Infrared and Raman Spectroscopy of Liquid Water through "First-Principles" Many-Body Molecular Dynamics. *J. Chem. Theory Comput.* **2015**, *11*, 1145−1154.
(22) Perakis, F.; Marco, L. D.; Shalit, A.; Tang, F.; Kann, Z. R.; Kuehne, T. D.; Torre, R.; Bonn, M.; Nagata, Y. Vibrational Spectroscopy and Dynamics of Water. *Chem. Rev.* **2016**, *116*, 7590−7607.
(23) Torii, H. Intermolecular Electron Density Modulations in Water and Their Effects on the Far-Infrared Spectral Profiles at 6 THz. *J. Phys. Chem. B* **2011**, *115*, 6636−6643.
(24) Torii, H. Cooperative Contributions of the Intermolecular Charge Fluxes and Intramolecular Polarizations in the Far-Infrared Spectral Intensities of Liquid Water. *J. Chem. Theory Comput.* **2014**, *10*, 1219−1227.
(25) Hasegawa, T.; Tanimura, Y. A Polarizable Water Model for Intramolecular and Intermolecular Vibrational Spectroscopies. *J. Phys. Chem. B* **2011**, *115*, 5545−5553.
(26) Ito, H.; Jo, J.-Y.; Tanimura, Y. Notes on simulating two-dimensional Raman and terahertz-Raman signals with a full molecular dynamics simulation approach. *Struct. Dyn.* **2015**, *2*, 054102.
(27) Ito, H.; Tanimura, Y. Simulating two-dimensional infrared-Raman and Raman spectroscopies for intermolecular and intramolecular modes of liquid water. *J. Chem. Phys.* **2016**, *144*, 074201.
(28) Tanimura, Y.; Mukamel, S. Two-dimensional femtosecond vibrational spectroscopy of liquids. *J. Chem. Phys.* **1993**, *99*, 9496−9511.
(29) Saito, S.; Ohmine, I. Off-resonant fifth-order response function for two-dimensional Raman spectroscopy of liquids CS_2 and H_2O. *Phys. Rev. Lett.* **2002**, *88*, 207401.
(30) Li, Y. L.; Huang, L.; Dwayne Miller, R. J.; Hasegawa, T.; Tanimura, Y. Two-dimensional fifth-order Raman spectroscopy of liquid formamide: Experiment and theory. *J. Chem. Phys.* **2008**, *128*, 234507.
(31) Frostig, H.; Bayer, T.; Dudovich, N.; Eldar, Y. C.; Silberberg, Y. Single-beam spectrally controlled two-dimensional Raman spectroscopy. *Nat. Photonics* **2015**, *9*, 339−343.
(32) Jo, J.-Y.; Ito, H.; Tanimura, Y. Full molecular dynamics simulations of liquid water and carbon tetrachloride for two-dimensional Raman spectroscopy in the frequency domain. *Chem. Phys.* **2016**, DOI: 10.1016/j.chemphys.2016.07.002.
(33) Hasegawa, T.; Tanimura, Y. Calculating fifth-order Raman signals for various molecular liquids by equilibrium and non-equilibrium hybrid molecular dynamics simulation algorithms. *J. Chem. Phys.* **2006**, *125*, 074512.
(34) Ito, H.; Hasegawa, T.; Tanimura, Y. Calculating two-dimensional THz-Raman-THz and Raman-THz-THz signals for various molecular liquids: The samplers. *J. Chem. Phys.* **2014**, *141*, 124503.
(35) Hamm, P.; Savolainen, J. Two-dimensional-Raman-terahertz spectroscopy of water: Theory. *J. Chem. Phys.* **2012**, *136*, 094516.
(36) Hamm, P.; Savolainen, J.; Ono, J.; Tanimura, Y. Note: Inverted time-ordering in two-dimensional-Raman-terahertz spectroscopy of water. *J. Chem. Phys.* **2012**, *136*, 236101.
(37) Savolainen, J.; Ahmed, S.; Hamm, P. Two-dimensional Raman-terahertz spectroscopy of water. *Proc. Natl. Acad. Sci. U. S. A.* **2013**, *110*, 20402−20407.
(38) Hamm, P. 2D-Raman-THz spectroscopy: A sensitive test of polarizable water models. *J. Chem. Phys.* **2014**, *141*, 184201.
(39) Ikeda, T.; Ito, H.; Tanimura, Y. Analysis of 2D THz-Raman spectroscopy using a non-Markovian Brownian oscillator model with nonlinear system-bath interactions. *J. Chem. Phys.* **2015**, *142*, 212421.
(40) Abascal, J. L. F.; Vega, C. A general purpose model for the condensed phases of water: TIP4P/2005. *J. Chem. Phys.* **2005**, *123*, 234505.
(41) Vega, C.; Abascal, J. L. F. Simulating water with rigid non-polarizable models: a general perspective. *Phys. Chem. Chem. Phys.* **2011**, *13*, 19663−19688.
(42) Bertie, J. E.; Lan, Z. D. Infrared Intensities of Liquids XX: The Intensity of the OH Stretching Band of Liquid Water Revisited, and the Best Current Values of the Optical Constants of H_2O(l) at 25°C between 15,000 and 1 cm^{-1}. *Appl. Spectrosc.* **1996**, *50*, 1047−1057.
(43) Brooker, M. H.; Hancock, G.; Rice, B. C.; Shapter, J. Raman Frequency and Intensity Studies of Liquid H_2O, $H_2^{18}O$ and D_2O. *J. Raman Spectrosc.* **1989**, *20*, 683−694.
(44) Khatib, R.; Hasegawa, T.; Sulpizi, M.; Backus, E. H. G.; Bonn, M.; Nagata, Y. Molecular dynamics simulations of SFG librational modes spectra of water at the water-air interface. *J. Phys. Chem. C* **2016**, *120*, 18665.

DOI: 10.1021/acs.jpclett.6b01766
J. Phys. Chem. Lett. 2016, 7, 4147−4151